ISSN No.: 2455-6130
Special Issue – RAISE2024, 2025, pp. 10-19

website: www.ijoetr.com

International Journal of Emerging Trends in Research

Strengthening Magnetic Behavior in M-type Ferrites via Al-Nd Co-substitution for Permanent Magnet Use

DeepikaSharma[1],Rohit[1], Vijay Singh[1], AnjanaDogra[2],andM. Singh[1]

[1]DepartmentofPhysics,HimachalPradeshUniversity,Shimla

[2](a)CSIR-NationalPhysicalLaboratory,Dr.K.S. Krishnan Marg,NewDelhi,India110012.
(b)AcademyofScientificandInnovativeResearch, (AcSIR),Ghaziabad,India201002

* Corresponding author. E-mail: deepika19399@gmail.com

Abstract

The growing need for permanent magnets in multiple sectors is hindered by the high expense of rare earth magnets, such as NdFeB. M-type strontium ferrite stands out as a practical substitute, offering both lower costs and excellent magnetic performance. This makes it a compelling option for numerous applications, including industrial motors, consumer electronics, renewable energy systems, and more. This study investigates the synthesis and characterization of Neodymium-Aluminum co-substituted M-type hexaferrite. Magnetic particles were synthesized using the sol-gel auto-combustion method. Structural analysis via XRD and HR-TEM confirmed the polycrystalline nature of the material. Increased doping concentrations resulted in a reduction of crystallite size from 104 nm to 61.33 nm (XRD). Magnetic measurements revealed that Al^{3+} and Nd^{3+} doping significantly enhanced coercivity form 5.5 kOe to 8 kOe. This improvement is attributed to the controlled reduction in particle size during synthesis. These results underscore the potential for enhancing magnetic properties by carefully regulating dopant levels in M-type hexaferrites, presenting them as promising substitutes for rare earth magnets.

Keywords:M-type Hexaferrite, Coercivity, Remanence, Electrical Vehicle

1. Introduction

The growing demand for high-performance permanent magnets, particularly in sectors like electric vehicles (EVs), renewable energy systems, and advanced electronics, has prompted significant interest in alternative materials that offer a balance between cost, availability, and magnetic performance. Rare-earth magnets, such as Neodymium Iron Boron (NdFeB) and Samarium Cobalt (SmCo), have traditionally dominated the market due to their superior magnetic properties, including

high remanence, coercivity, and energy product. However, the high cost, environmental concerns, and uneven distribution of rare-earth elements have spurred research into more sustainable and economically viable alternatives[1–4]. Among these, M-type hexagonal ferrites ($MFe_{12}O_{19}$, where M = Ba, Sr, or Pb) have emerged as promising candidates for permanent magnet applications. Discovered by Philips Research Laboratories in 1952, M-type ferrites are widely recognized for their affordability, chemical stability, mechanical strength, and ease of synthesis. Though they offer lower remanent magnetization (M_r) and coercivity (H_c) compared to rare-earth magnets, their unique properties, including high Curie temperatures, uniaxial anisotropy, and low eddy current losses, make them ideal for various applications such as magneto-optical systems, microwave devices, recording media, radiation shielding, and sensors. The material cost-effectiveness and abundance position them as attractive substitutes for rare-earth magnets, particularly in EV motors, where achieving a balance between high magnetic strength and resistance to demagnetization is crucial[5–7].

The magnetic properties of this ferrite material are closely linked to its crystal structure, which is extensively studied to understand and explain its behaviour. M-type ferrites share a structural similarity with the magneto-plumbite structure, characterized by significant magneto-crystalline anisotropy along their crystallographic axis, which provides high coercivity and strong resistance to demagnetization. The hexagonal unit cell of strontium ferrite contains two formula units, each consisting of 32 atoms, totaling 64 atoms per cell. The structure is composed of tightly packed Sr^{2+} and O^{2-} ions, with Fe^{3+} ions positioned in various sites. These include one tetrahedral site, two FeO_4 ($4f_1$) sites, one triangular bipyramidal FeO_5 (2b) site, and three octahedral FeO_6 sites (2a, 12k, $4f_2$). The magnetic interactions between the 24 Fe^{3+} ions in five different sites are mediated by super exchange interactions through O^{2-}. The magnetic moment arises from Fe^{3+} ions, each contributing $5\mu_B$, with 8 spin-up Fe ions located at the 2a, 12k, and 2b sites, and 4 spin-down Fe ions at the $4f_1$ and $4f_2$ sites, yielding a total magnetic moment of 20 μ_B[8].

Cation substitution in M-type hexaferrites can be used to tailor their magnetic properties. For example, Nd substitution can enhance remanent magnetization (M_r), while Al doping increases coercivity (Hc) but may reduce remanence. In Nd-substituted $Sr_{1-x}Nd_xFe_{12}O_{19}$, Hc initially rises with Nd content up to x = 0.08, after which it declines, while Ms and Mr remain nearly constant[9]. Numerous research papers demonstrate the H_c improves when doped with aluminiumions[10–14]. Luo et al. conducted a study on Al-doped M-type ferrite $SrFe_{12-x}Al_xO_{19}$ ($0 < x < 12$) and demonstrated that the coercivity (Hc) depends on the Al^{3+} doping concentration, peaking at 18.1 kOe when x = 4, but rapidly decreasing beyond this point. While the increase in Hc is comparable to that of expensive rare-earth magnets, the drawback is a significant reduction in remanence at higher coercivity levels. [14]. Chang et al. investigated the Nd-Co co-doped M-type hexaferrite ($Nd_xSr_{1-x}Co_xFe_{12-x}O_{19}$, x = 0.00–1.00) and reported that the coercivity increased from 3353.00 to 4045.20 Oe when $x < 0.20$. Saturation magnetization decreased from 64.39 to 62.73 emu/g, a 2.58% decrease [15]. Yang et al. studied M-type hexaferrites that were synthesized by the conventional ceramic process and had the chemical composition $Ca_{0.4}Sr_{0.6-x}Pr_xFe_{12.0-y}Al_yO_{19}$ ($0.00 \le x \le 0.40$, $0.00 \le y \le 0.60$). The $(BH)_{max}$ and M_r diminish as the Pr-Al concentration rises ($0.00 \le x \le 0.40$, ($0.00 \le y \le 0.60$). With a rising Pr-Al concentration ($0.00 \le x \le 0.40$, ($0.00 \le y \le 0.60$), the intrinsic coercivity (H_{cj}) rises [16].

In this study, we explore the potential of M-type hexaferrites for permanent magnet applications by investigating the effects of cation substitution on their magnetic properties. Specifically, we focus on Nd and Al co-substitution in Sr-hexaferrites, aiming to enhance Hc while maintaining or improving M_r and M_s. This investigation addresses a key gap in the literature and provides valuable insights into

the structural and magnetic behaviour of Nd-Al co-substituted M-type hexaferrites, with implications for their application in next-generation permanent magnets. Thereby, using the conventional sol-gel approach, we succeeded in effectively synthesizing Nd-Al co-substituted ($Sr_{1-x}Nd_xAl_yFe_{12-y}O_{19}$ $0.00<x<0.20$, $0.00<y< 2.00$) M-type hexaferrites in this work.

2. preparations route

The auto-combustion sol-gel method was used to synthesize $Sr_{1-x}Nd_xAlyFe_{12-y}O_{19}$ ($0.00<x<0.20$, $0.00<y<2.00$) ferrites using nitrate salts of Sr, Nd, Fe, and Al, with citric acid as a chelating agent and ethylene glycol as a surfactant. The solution was stirred continuously, and ammonia was added to adjust the pH to 8-9. The mixture was heated to 80°C to promote the formation of magnetic particles, and the resulting powder was ground and calcinated at 1100°C for 4 hours. The prepared powder was then analyzed for structural and magnetic properties.

The chemical route followed by the equations are:

$$(1\text{-}X)\ .Sr(NO_3)_2 + X.Nd(NO_3)_2 + (12\text{-}y)Fe(NO_3)_2 + y.\ Al(NO_3)_2 + C_6H_8O_7 + NH_4OH \rightarrow Sr_{1-x}Nd_xAl_yFe_{10-y}O_{19} + NH_4NO_3 + CO_2 + H_2O$$

Table 1 : Formula of samples A, B and C

Sample Name	Chemical Formula
A	$SrFe_{12}O_{19}$
B	$Sr_{0.90}Nd_{0.10}Fe_{11.00}Al_{1.00}0_{19}$
C	$Sr_{0.80}Nd_{0.20}Fe_{10.00}Al_20_{19}$

Figure 1: Auto-combustion sol-gel method for the preparation of M-type nano

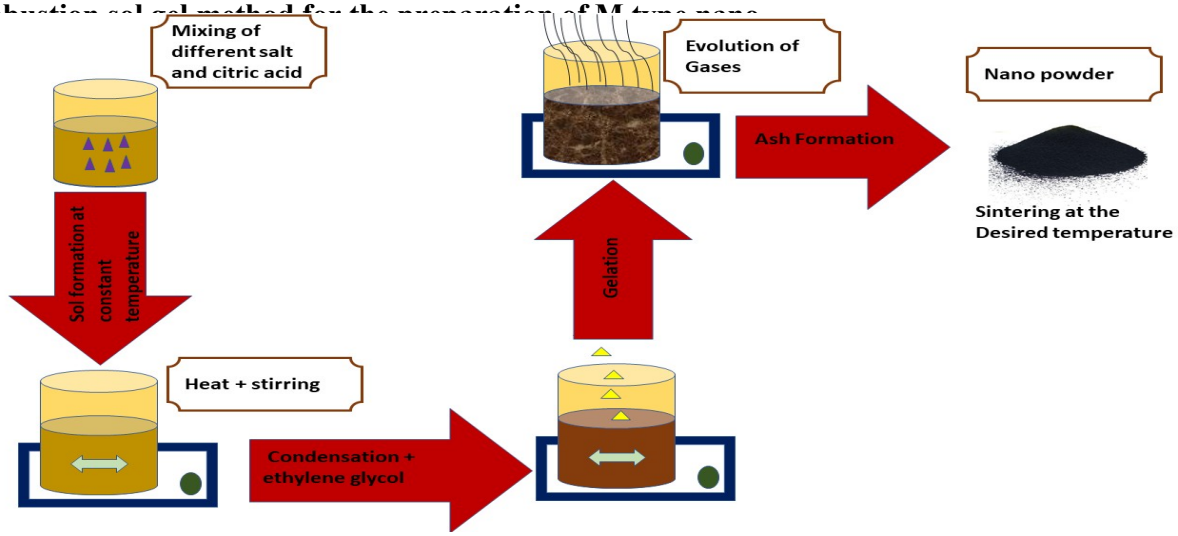

hexaferritesamples[17]

3. Results and Discussion

3.1. Structural study

XRD:

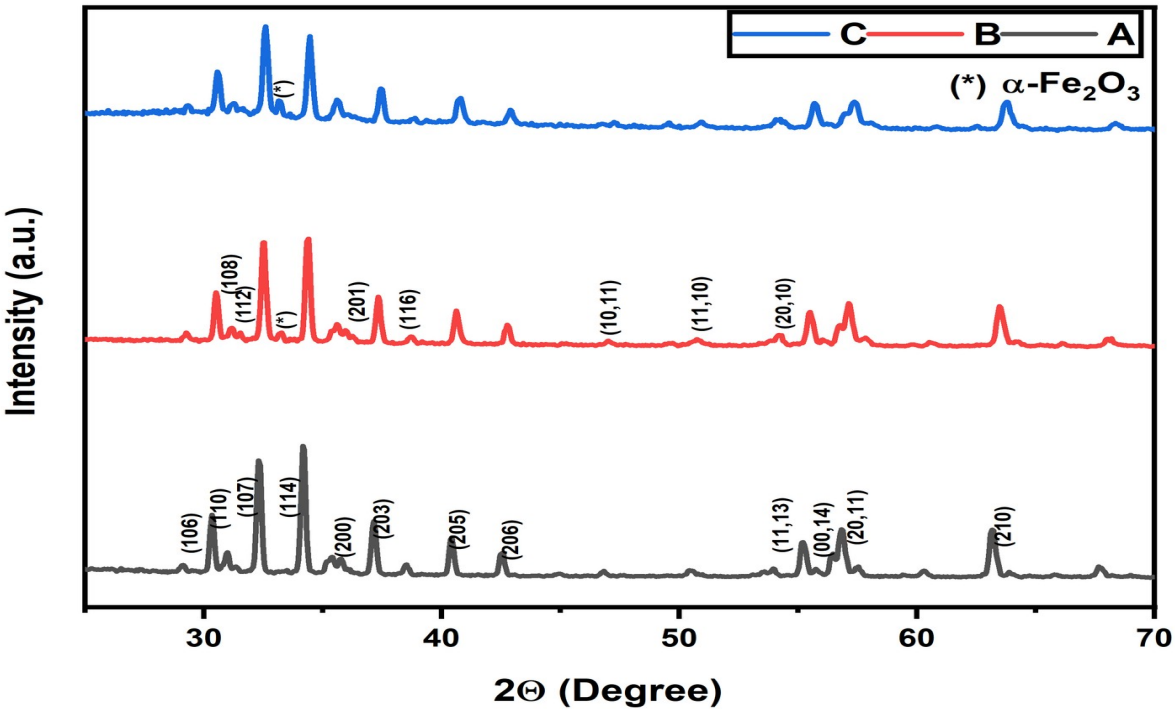

Figure 2: X-Ray Diffraction Pattern for the Nd-Al doped samples $Sr_{1-x}Nd_xAl_yFe_{12-y}O_{19}$ (0.00<x<0.20, 0.00<y< 2.00) Named as "A, B and C "

The XRD patterns of samples "A" , "B", and "C" confirm the polycrystalline nature of M-type strontium hexaferrite, as indicated by ICCD card no. 80-1198. For sample "B" and "C" with Nd–Al content (x = 0.20), the dominant phase remains M-type hexaferrite, but low-intensity impurity phases of hematite (α-Fe_2O_3) emerge, corresponding to ICCD card no. 87-1166. Lattice parameters "a" and "c" and unit cell volume (V_{cell}) were calculated using Bragg's equation for interplanar spacing (d_{hkl}) and unit cell volume equations [18].

$$d_{hkl} = \frac{1}{\sqrt{\frac{4\left(h^2+hk+k^2\right)}{3a^2}+\frac{l^2}{c^2}}} \quad (1)$$

$$V_{cell} = \frac{\sqrt{3}}{2} a^2 c \quad (2)$$

The lattice parameters for the pure and Nd-Al doped hexaferrites are shown in Table 2. As the concentration of the doping material increases, both the lattice parameters and the unit cell volume decrease. This contraction is attributed to the difference in the ionic radii of the substituent ions. Nd^{3+} (r = 0.983 Å) replacing Sr^{2+} (r = 1.180 Å)[19] and Al^{3+} (r = 0.535 Å) replacing Fe^{3+} (r = 0.645 Å) [14] result in negative variations in the ionic radii, with Δr values of -0.197 Å and -0.11 Å, respectively. For samples "A," "B," and "C," there is a decrease in the lattice parameters "a" and "c" as doping

concentration increases. The values show a contraction of 0.85%, 0.90%, and 2.6% in "a," "c," and the unit cell volume, respectively, indicating that the c-axis contracts more than the a-axis. Crystallite size for each sample was determined using the Scherrerformula[20] as given below, confirming the nanoscale structure of the synthesized ferrites.

$$D = \frac{K\lambda}{\beta COS\Theta}$$

Table 1 Lattice parameter, c/a ratio, cell volume and crystallite size calculated via X-ray Diffraction Pattern

Sample Name	a (Å)	c (Å)	c/a	Volume (Å ^3)	Crystallite Size (nm)
A	5.87	23.02	3.92	687.89	104
B	5.85	22.92	3.91	679.67	68.28
C	5.82	22.81	3.91	669.58	61.33

HR-TEM:

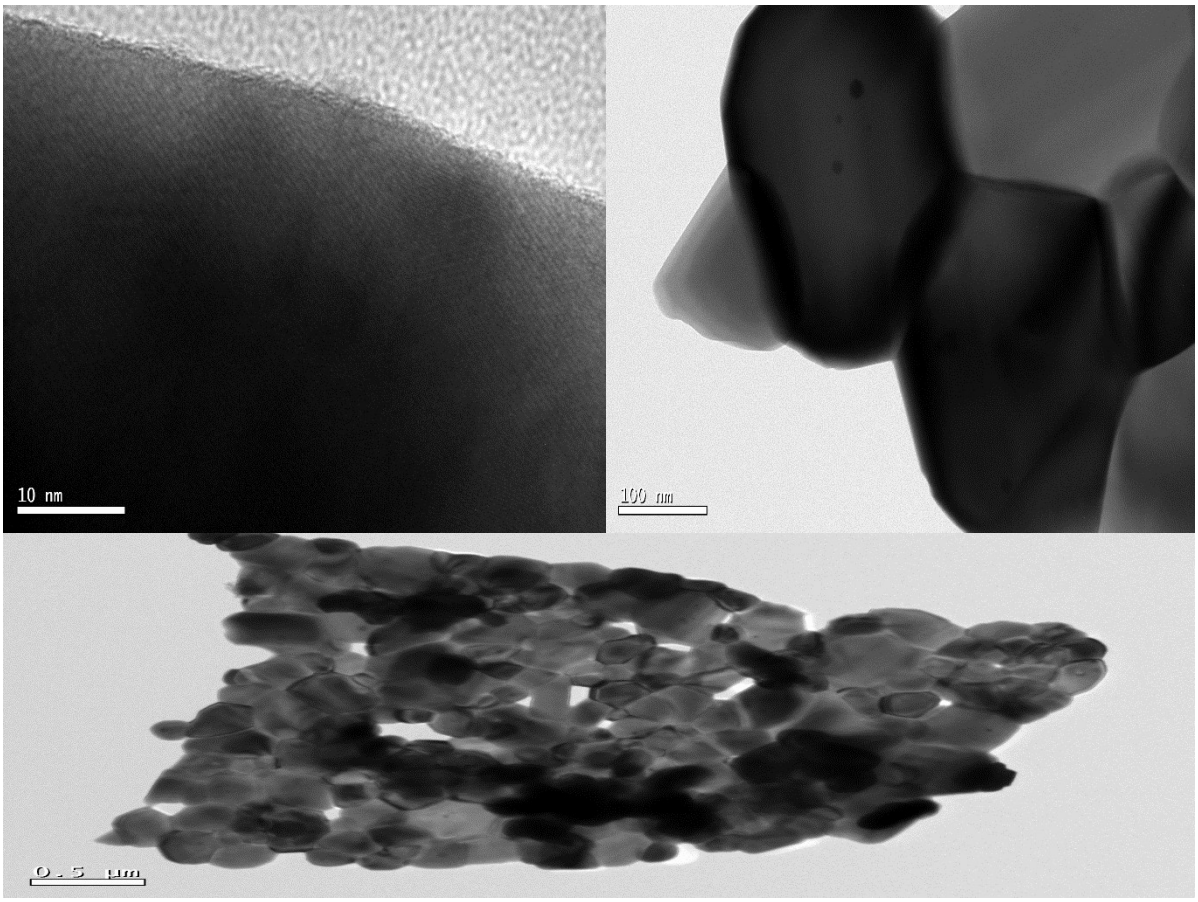

Figure 3: HR-TEM images of the M type ferrite samples

Figure 3 shows the HR-TEM micrographs of the fabricated ferrite samples provide structural insights, showing agglomerated particles with varied morphologies, including spherical, hexagonal, and irregular shapes. The TEM analysis confirms the formation of these distinct particle shapes, and the structural details align well with the data obtained from XRD, supporting the overall findings on the ferrite samples

3.2. Magnetic study

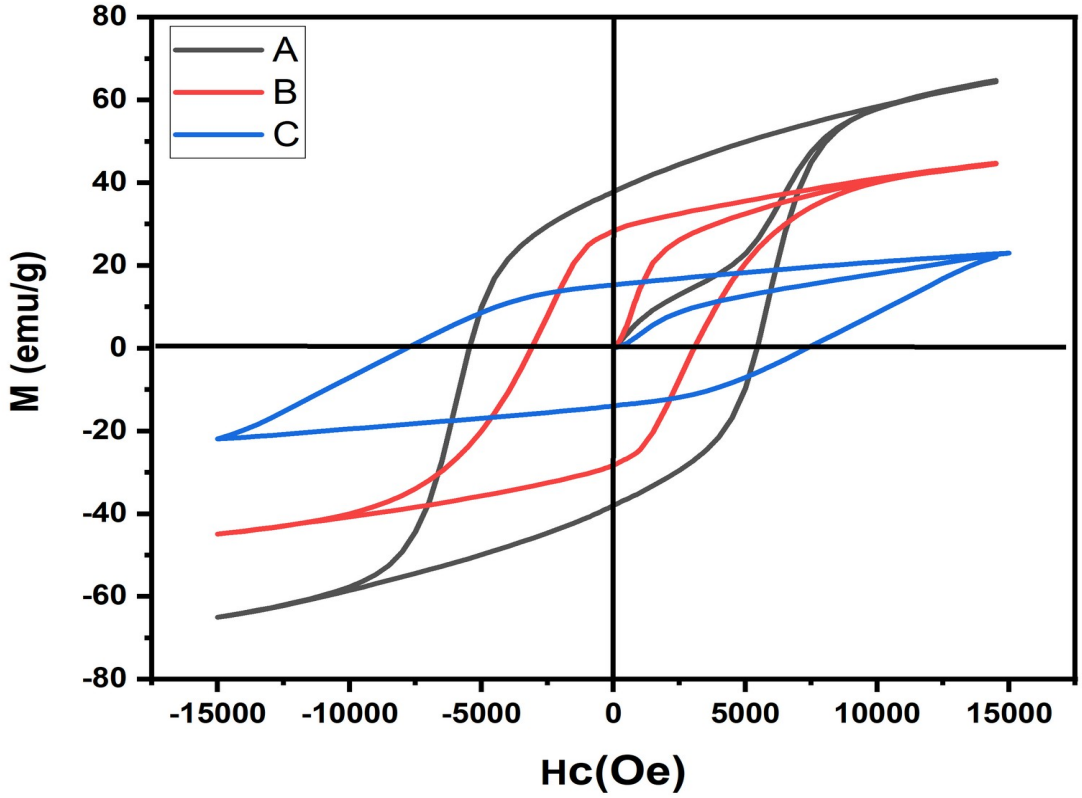

Figure 4: Hysteresis loop for pure and Nd-Al doped M-type hexaferrite samples named as A,B and C

Fig. 4 illustrates the hysteresis loop characteristics of the $Sr_{1-x}Nd_xAl_yFe_{10-y}O_{19}$ ($0.00<x<0.20$, $0.00<y<2.00$) samples in powdered form at room temperature (RT), highlighting their ferromagnetic nature. The samples exhibit distinct localized hysteresis behaviour, confirming their strong magnetic characteristics at RT under a magnetic field intensity of 15 kOe. Sample "A" shows the high value of H_c and M_r, with Hc = 5.5 kOe and M_r = 39.29 emu/g. These values align well with or exceed those reported for M-type strontium hexaferrite in earlier studies [13, 21][17].

Table 3: Saturation magnetization M_S (emu/g), Remanent magnetization M_r (emu/g), Coercivity H_c (KOe), squareness ratio M_r/M_s of pure and Nd-Al doped M-type hexaferrite samples

Sample Name	M_S (emu/g)	M_r (emu/g)	H_c(KOe)	M_r/ M_S
A	64.40	39.29	5.5	0.61
B	44.57	29.55	3.57	0.66
C	23.01	15.61	8.00	0.67

In terms of magnetic properties, the incorporation of Nd^{3+} and Al^{3+} ions affect the samples' saturation magnetization, remanence, and coercivity. As the doping content increases, the values of M_s and M_r decrease. In sample "B" , the coercivity drops to 3.57 kOe, and the remanent magnetization decreases to 29.55 emu/g compared to sample “A”. The decrease in M_r and M_s of the ferrite can be attributed to the substitution of Fe^{3+} ions, which possess a magnetic moment of 5 μ_B, with diamagnetic Al^{3+} ions at specific crystallographic sites where spins are predominantly aligned upwards, especially at the 12k sites [14]. This substitution weakens the super-exchange interaction between Fe^{3+}-O-Fe^{2+} pairs, leading to a reduction in both M_s and M_r. Additionally, this decline in exchange interactions causes a non-collinear spin configuration.Furthermore, Mossbauer spectroscopy indicates that surface defects in nanocrystalline $SrFe_{10.5}Al_{1.5}O_{19}$ contribute to the reduction in exchange interactions, further lowering the overall magnetization[14, 22]. The substitution of Al^{3+} ions also mirrors the effects seen in previous studies involving Al-Ga substitutions in similar hexaferrites[23, 24]. Similarly, the replacement of Sr^{2+} with Nd^{3+} can induce a valence change in Fe ions at the 2a or $4f_2$ sites, potentially decreasing the Ms values due to the alteration of magnetic interactions at these specific sites[25, 26].

Sample "C" shows a significant increase in coercivity (H_c = 8.0 kOe) and a substantial reduction in remanence (M_r = 15.61 emu/g). The increment in coercivity of the ferrite with Al doping can be attributed to two main factors: the critical size for single-domain particles and the magneto-crystalline anisotropy of the material [27]. As the amount of Al doping increases, the single-domain limit rises, which, along with a reduction in grain size, restricts the movement of the domain walls. This hindrance in domain wall mobility leads to an increase in coercivity[27]. Additionally, the rise in magneto-crystalline anisotropy, particularly in the higher Al-doped samples, contributes to this increase, further enhancing the material's resistance to demagnetization. This behaviour highlights the delicate balance between ion substitution and magnetic properties, with doping levels having a profound impact on the material's coercive and magnetic behaviour.

4. Conclusion

In this study, the structural and magnetic properties of Nd-Al co-substituted M-type Srhexaferrites, $Sr_{1-x}Nd_xAl_yFe_{10-y}O_{19}$ ($0.00<x<0.20$, $0.00<y<2.00$), were systematically investigated. X-ray diffraction analysis confirmed the successful synthesis of hexagonal ferrite structures, with no secondary phase detected, indicating the stability of the material upon doping. The incorporation of Nd^{3+} and Al^{3+} ions led to significant changes in both the microstructure and magnetic behaviour. As the doping levels increased, there was a clear trend of decreasing saturation magnetization and remanent magnetization particularly due to the substitution of Fe^{3+} ions by diamagnetic Al^{3+} ions at specific crystallographic sites, such as 12k. H_c initially decreased but exhibited a sharp rise at higher doping concentrations, with the highest value observed for sample C ($Sr_{0.8}Nd_{0.2}Al_{1.0}Fe_{11}O_{19}$). The study offers a promising avenue for further exploration, particularly in optimizing the magnetic properties through precise control of Nd and Al doping levels. Adjusting the doping amount could potentially lead to materials with tailored coercivity and magnetization, making them suitable for specific applications in magnetic storage devices, permanent magnets, and energy-efficient electric vehicle (EV) motors. Future work may involve a deeper exploration of the relationship between doping concentrations and domain wall behaviour, as well as investigating other potential dopants to further enhance the magnetic performance of these hexaferrites.

References

[1] Moon KS, Lim ES, Kang YM (2019) Effect of Ca and La substitution on the structure and magnetic properties of M-type Sr-hexaferrites. J Alloys Compd 771, 350–355.

[2] Kobayashi Y, Hosokawa S, Oda E, Toyota S (2008) Magnetic properties and composition of Ca-La-Co M-type ferrites. FuntaiOyobiFunmatsuyakin 55,541–546

[3] Kools F, Morel A, Grössinger R, et al (2002) LaCo-substituted ferrite magnets, a new class of high-grade ceramic magnets; intrinsic and microstructural aspects. J MagnMagn Mater 242–245,1270–1276.

[4] Iida K, Minachi Y, Masuzawa K, et al (1999) High - Performance Ferrite Magnets: M - Type Sr - Ferrite Containing Lanthanum and Cobalt. Journal of the Magnetics Society of Japan 23, 1093–1096.

[5] Deshpande AD, Rewatkar KG, Nanoti VM (2017) Study of Morphology and Magnetic Properties of Nanosized Particles of Zirconium – Cobalt Substituted Calcium Hexaferrites. Mater Today Proc 4, 12174–12179.

[6] Thakur M, Singh C, Martinson KD, et al (2023) Significantly improved magnetic parameters of Co–La co-doped strontium hexagonal ferrites for recording applications: structural, hysteresis, and mössbauer performance metrics. Journal of Materials Science: Materials in Electronics 34, 1–20

[7] Bayrakdar H (2016) Fabrication, magnetic and microwave absorbing properties of Ba2Co2Cr2Fe12O22 hexagonal ferrites. J Alloys Compd 674, 185–188.

[8] Verma A, Pandey O, Sharma P (2000) Strontium ferrite permanent magnet-an overview. Indian Journal of Engineering and Materials Sciences (IJEMS 7, 364–369

[9] Mocuta H, Lechevallier L, Le Breton JM, et al (2004) Structural and magnetic properties of hydrothermally synthesised Sr1−xNdxFe12O19 hexagonal ferrites. J Alloys Compd 364, 48–52.

[10] Ijaz M, Ullah H, Ali Al-Asbahi B, et al (2024) Co-precipitation method followed by ultrafast sonochemical synthesis of aluminium doped M type BaFe11.4-xAlxCo0.6O19 hexaferrites for various applications. J MagnMagn Mater 589, 171559.

[11] Dogra A, Singh M, Kumar R (2003) 50 MeV Li3+ ion irradiation induced modifications in dielectric properties of Al3+ substituted Mg-Mn ferrite. NuclInstrum Methods Phys Res B 207, 296–300.

[12] Gupta A, Roy PK (2023) Effect of Zn2+ ion substitution in Al3+-substituted rare-earth free Sr-hexaferrite for different permanent magnet applications. InorgChemCommun 155, 111-114.

[13] Li P, Li J, Wang Y, et al (2023) Structural, Spectral, and Magnetic Properties of Praseodymium–Aluminum-Co-doped M-Type Barium Hexaferrites. J Supercond Nov Magn 36:327–341.

[14] Luo H, Rai BK, Mishra SR, et al (2012) Physical and magnetic properties of highly aluminum doped strontium ferrite nanoparticles prepared by auto-combustion route. J MagnMagn Mater 324, 2602–2608.

[15] Chang X, Xiong Z, Wang R, et al Study on electrical and magnetic properties of Nd-Co co-substituted M-type strontium ferrite suitable for microwave devices. Journal of Materials Science: Materials in Electronics 34.

[16] Yang Y, Liu X, Feng S, et al (2020) Effects of Pr-Al co-substitution on the magnetic and structural properties of M-type Ca-Srhexaferrites. Chinese Journal of Physics 63, 337–347.

[17] Sharma D, Rohit, Singh V, et al (2024) Aluminium and praseodymium doped M-type hexaferrites for electric vehicle applications. Ceram Int 50, 24815–24822.

[18] Xu J, Ji G, Zou H, et al Structural, dielectric and magnetic properties of Nd-doped Co2Z-type hexaferrites. Elsevier

[19] Yang Y, Wang F, Shao J, et al (2018) Influence of Nd-NbZn co-substitution on structural, spectral and magnetic properties of M-type calcium-strontium hexaferrites Ca0.4Sr0.6-xNdxFe12.0-x(Nb0.5Zn0.5)xO19. J Alloys Compd 765, 616–623.

[20] Yousaf M, Nazir S, Hayat Q, et al (2021) Magneto-optical properties and physical characteristics of M-type hexagonal ferrite (Ba1-xCaxFe11.4Al0.6O19) nanoparticles (NPs). Ceram Int 47, 11668–11676.

[21] Li P, Li J, Wang Y, et al (2023) Structural, Spectral, and Magnetic Properties of Praseodymium–Aluminum-Co-doped M-Type Barium Hexaferrites. J Supercond Nov Magn 36, 327–341.

[22] Singh J, Singh C, Kaur D, et al (2016) Elucidation of phase evolution, microstructural, M € ossbauer and magnetic properties of Co 2þ eAl 3þ doped M-type BaeSrhexaferrites synthesized by a ceramic method.

[23] Iqbal MJ, Ashiq MN, Hernandez-Gomez P, Munoz JM (2008) Synthesis, physical, magnetic and electrical properties of Al–Ga substituted co-precipitated nanocrystalline strontium hexaferrite. J MagnMagn Mater 320, 881–886.

[24] Dhage VN, Mane ML, Keche AP, et al (2011) Structural and magnetic behaviour of aluminium doped barium hexaferrite nanoparticles synthesized by solution combustion technique. Physica B Condens Matter 406, 789–793.

[25] Herme CA, Bercoff PG, Jacobo SE (2012) Nd–Co substituted strontium hexaferrite powders with enhanced coercivity. Mater Res Bull 47, 3881–3887.

[26] Yang Y, Wang F, Shao J, et al (2018) Influence of Nd-NbZn co-substitution on structural, spectral and magnetic properties of M-type calcium-strontium hexaferrites Ca0.4Sr0.6-xNdxFe12.0-x(Nb0.5Zn0.5)xO19. J Alloys Compd 765, 616–623.

[27] Luo H, Rai BK, Mishra SR, et al (2012) Physical and magnetic properties of highly aluminum doped strontium ferrite nanoparticles prepared by auto-combustion route. J MagnMagn Mater 324, 2602–2608.